Journal of Physics: Conference Series **160** (2009) 012012 doi:10.1088/1742-6596/160/1/012012

The ALICE Electromagnetic Calorimeter Project

F. Ronchetti, on behalf of the ALICE collaboration.

Istituto Nazionale Fisica Nucleare,
Laboratori Nazionali di Frascati
Via E. Fermi 40
00044 Frascati (Roma)

Federico.Ronchetti@LNF.INFN.IT

Abstract. The ALICE Experiment (A Large Ion Collider Experiment) aims to study the properties of quark-gluon matter using Pb-Pb collisions at a center of mass energy (per nucleon pair) of $\sqrt{s_{NN}}$ = 5.5 TeV with the Large Hadron Collider (LHC) at CERN. The EMCal consists in a large area electromagnetic calorimeter able to extend the measured momentum range of photons and electrons by over an order of magnitude. In addition, the EMCal will enhance the capability of the overall ALICE setup to perform better jet reconstruction by measurement of the neutral energy component of jets, photons and neutral pions. The EMCal will also produce a fast high-p_T trigger: the anticipated minimum bias average Pb-Pb interaction rate is very high (around 8 kHz), thus a fast high-p_T trigger will provide an enhancement in high p_T events in central collisions. The EMCal covers a geometrical region from $-0.7 \leq \eta \leq 0.7$ (in pseudo-rapidity η) and 120° in the azimuthal angle ϕ. In particular, the ϕ-coverage has been chosen to allow the detection of γ-jet events in coincidence with the other ALICE complementary calorimeter, the PHOS. The EMCal is a modular sampling calorimeter: it can measure showers up to 20 radiation lengths. Each module is composed by 4 towers of a Pb-scintllator sandwich (shashlik). The shape of the basic module is tapered to allow a projective geometry of the final assembly with respect to the interaction point. An assembly of 12×24 modules is called a super-module. The complete EMCal is a high granularity detector containing 11 super modules for a total of 12.672 towers. An independent optical readout of each tower is provided using wavelength shifting fibers coupled to an APD (Avalanche Photo Diod). The APD readout was chosen to allow the operation in the high B-field environment created by the ALICE solenoidal magnet. The gain of the APD is monitored using a LED activated scintillator installed on into each module.

1. Introduction

1.1. Physical motivation

The ALICE experiment at LHC is made out of a wide array of detector systems for measuring hadrons, leptons, and photons. ALICE is designed to carry out comprehensive measurements of high energy nucleus-nucleus collisions, in order to study QCD matter under extreme conditions and to study the phase transition between condensed matter and the Quark-Gluon Plasma (QGP) [1,2]. The interaction and energy loss of high energy partons in matter provides a sensitive tomographic probe of the medium generated in high energy nuclear collisions (jet quenching) [3-6]. Jet quenching measurements have played a key role at the Relativistic Heavy Ion Collider (RHIC) and will be central to the study of nuclear collisions at LHC. The EMCal enhances ALICE's capabilities for jet quenching

measurements. The addition of the EMCal into ALICE enables triggering on high energy jets, reduces significantly the measurement bias for jet quenching studies, improves jet energy resolution, and augments existing ALICE capabilities to measure high momentum photons and electrons. Combined with ALICE's excellent capabilities to track and identify particles from very low p_T to high p_T, the EMCal enables an extensive study of jet quenching at the LHC.

1.2. The ALICE Electromagnetic Calorimeter

ALICE is designed for measurements in the high multiplicity environment of heavy ion collisions and is well suited for jet quenching studies. It has excellent momentum resolution for charged particles from 100 MeV/*c* to 100 GeV/*c*, covering nearly the full range of fragment momentum for the highest energy jets accessible in heavy ion collisions. The EMCal will complete ALICE's capabilities to measure jet quenching. The most important features of the EMCal are an efficient and unbiased fast trigger (Level 0/1) for high energy jets, and measurement of the neutral portion of jet energy. The EMCal will also improve jet energy resolution, and enhance ALICE capabilities to measure high p_T photons, neutral hadrons, and electrons.

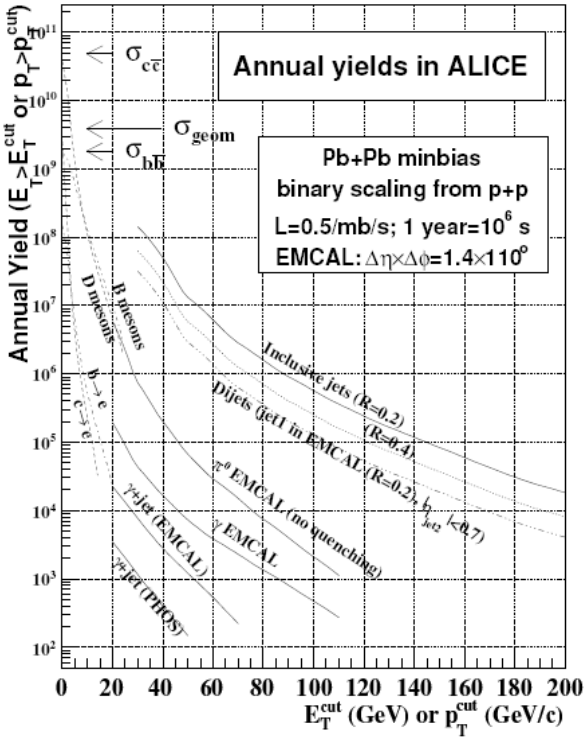

Figure 1: Annual hard process yields in the EMCal acceptance for minimum bias Pb-Pb collisions at 5.5 TeV.

Fig. 1 shows the annual yield for various hard processes in the EMCal acceptance, for minimum bias Pb-Pb collisions at nominal luminosity. The EMCal kinematic reach for inclusive jets extends beyond 200 GeV, while for di-jets with a trigger jet in the EMCal and the recoiling jet in the TPC acceptance it is about 170 GeV. The γ-jet rate is statistically robust for $p_T \leq 40$ GeV/*c*, while the yield for inclusive electrons from semi-leptonic decays of *b* and *c* extends to $p_T \sim 25$ GeV/*c*.

ALEPH [7] and STAR [8] have shown that jet measurements based on electromagnetic calorimetry and charged particle tracking have similar energy resolution to e.m. and hadronic calorimetry. In fact, charged particle tracking is superior to hadronic calorimetry for suppressing backgrounds to jet measurements in the high multiplicity environment of heavy ion collisions. Full exploitation of jets as a probe of QCD matter at the LHC requires both broad kinematic reach of jet energy and detailed measurement of jet structure, from the hardest hadronic fragments to very soft fragments. Much of the interesting physics may indeed be carried by low p_T hadrons, which have the greatest sensitivity to the jet interaction with the medium. From the experience of RHIC measurements [9,10], particle identification is expected to be critical in elucidating the physics of jet quenching. The EMCal acceptance, triggering and measurement capabilities, combined with the excellent tracking and particle identification capabilities of ALICE, enable the most extensive measurements of jet quenching at the LHC.

2. Detector design

2.1. Design overview.

The overall design of the EMCal is heavily influenced by its integration within the ALICE magnet. The EMCal is to be located inside the large room temperature solenoidal magnet of ALICE within a cylindrical integration volume approximately 112 cm deep in the radial direction, sandwiched between the ALICE spaceframe and the ALICE magnet coils. Due to the presence of the PHOS carriage below the ALICE TPC and the HMPID above the ALICE TPC, the EMCal covers a region of about 110 degrees in azimuth above the TPC adjacent to the HMPID and its acceptance is well matched to ALICE physics goals.

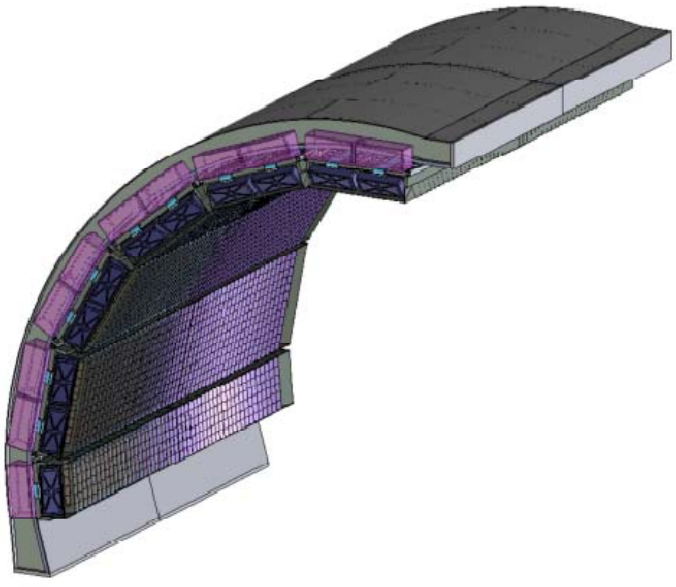

Figure 2: The array of super modules shown in the installed position on their support structure.

The conceptual design of the electromagnetic calorimeter for the ALICE experiment is based on the Shashlik technology as implemented in the PHENIX experiment [11] at RHIC, HERA-B at DESY or LHCb [12] at CERN. The scope and basic design parameters of the proposed calorimeter have been chosen to match the physics performance requirements of the high p_T physics program. Fig. 2 shows the EMCal super modules mounted in the installed position on their support structure. A continuous arch of super modules, each spanning ~20 degrees in azimuth, is indicated. The EMCal is positioned

to provide partial back-to-back coverage with the ALICE Photon Spectrometer (PHOS) calorimeter. Small azimuthal gaps (~ 3.0 cm) are provided between super modules to facilitate installation and alignment. These gaps are positioned in line with the TPC sector boundaries. The chosen technology is a layered Pb-scintillator sampling calorimeter with a longitudinal pitch of 1.44 mm Pb and 1.76 mm scintillator with longitudinal Wavelength Shifting Fiber (WLS) light collection. The full detector spans $\eta = -0.7$ to $\eta = 0.7$ with an azimuthal acceptance of $\Delta\phi = 110$. The detector is segmented into 12,672 towers, each of which is approximately projective in η and ϕ to the interaction vertex. The towers are grouped into super modules of two types: full size which span $\Delta\eta = 0.7$ and $\Delta\phi = 20$ and half size which span $\Delta\eta = 0.7$ and $\Delta\phi = 10$. There are 10 full size and 2 half size super modules in the full detector acceptance (Fig. 2). The super module is the basic structural units of the calorimeter. These are the units handled as the detector is moved below ground and rigged during installation.

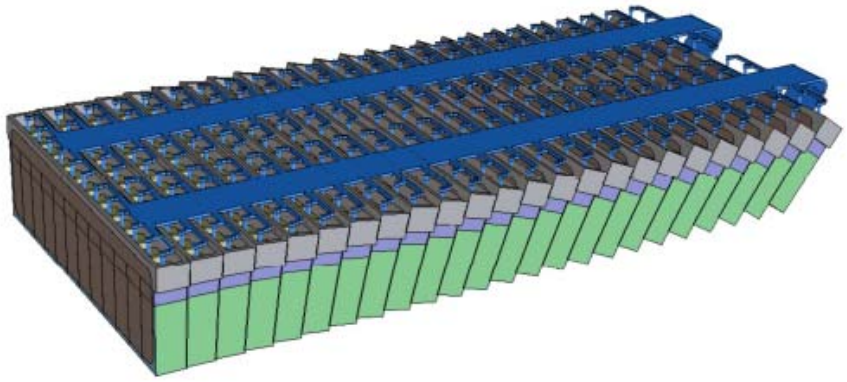

Figure 3: ALICE EMCal super module concept.

Fig. 3 shows a super module with its external mechanical structure stripped away to illustrate the stacking of modules within the super module. This figure shows a full size super module with 12× 24 modules configured as 24 strip modules of 12 modules each. The supporting mechanical structure of the super module has been removed so that the strip module stacking into a nearly projective geometry can be seen. The electronics integration pathways are illustrated. Each full size super module is assembled from $12 \times 24 = 288$ modules arranged in 24 strip modules of 12 modules each. Each module has a rectangular cross section in the ϕ direction and a trapezoidal cross section in the η direction with a full taper of 1.5°. The resultant assembly of stacked strip modules is approximately projective with an average angle of incidence of less than 2° in η and less than 5° in ϕ. A single module and an assembled strip module is indicated schematically in Fig. 4.

2.2. Module Design

The smallest building block of the calorimeter is the individual module illustrated in Fig. 4. Each individual module contains $2 \times 2 = 4$ towers built up from 77 alternating layers of 1.44 mm Pb and 1.76 mm polystyrene, injection molded scintillator. White, acid free, bond paper serves as a diffuse reflector on the scintillator surfaces while the scintillator edges are treated with TiO_2 loaded reflector to provide tower to tower optical isolation and improve the transverse optical uniformity within a single tower. The Pb-scintillator stack in a module is secured in place by the static friction between individual layers under the overall load of ~350 kg. The module is closed by a skin of 150 μm thick stainless steel screwed by flanges on all four transverse surfaces to corresponding front and rear aluminum plates. This thin stainless skin is the only inert material between the active tower volumes. The internal pressure in the module is stabilized against thermal effects, mechanical relaxation and long term flow of the Pb and/or polystyrene by a customized array of 5 non-linear spring sets

(Bellville washers) per module. In this way, each module is a self supporting unit with a stable mechanical lifetime of more than 20 years when held from its back surface in any orientation as when mounted in a strip module.

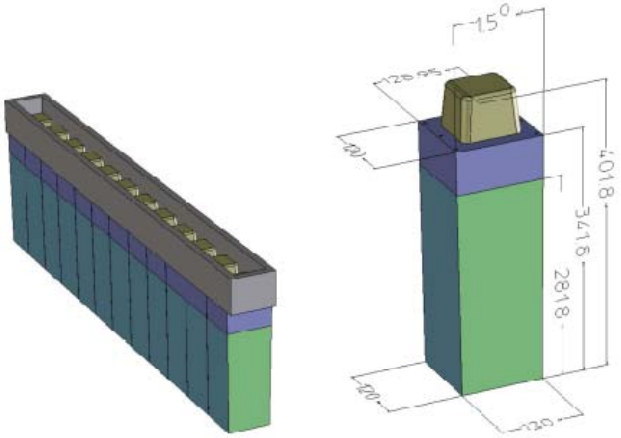

Figure 4: A single 1.5° taper module (right hand side) with the dimensions of the prototype shown in mm. The left hand figure shows a single strip module comprised of 12 EMCal modules integrated onto a single strong back.

Fig. 5 below shows a cut away view of the back end of a single module illustrating the internal components used to sustain the module compression and a segment of the strip module strong back.

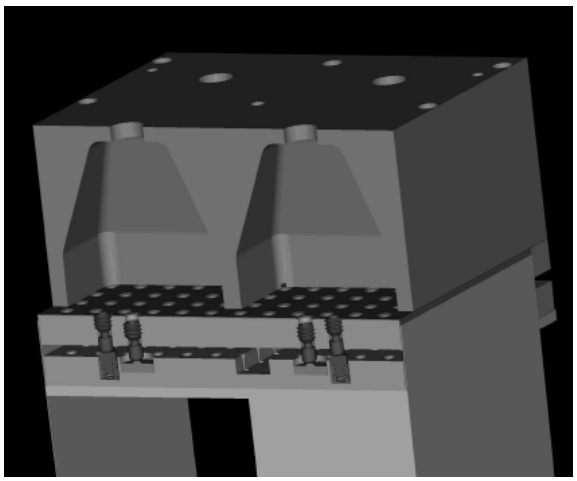

Figure 5: Cut away view of the back end of a single module showing the components that maintain the module's compression. The Bellville washers act between the two containment Al plates to keep the module internal load. A segment of the strip module strong back is also shown.

All modules in the calorimeter are mechanically and dimensionally identical. The front face dimensions of the towers are 6×6 cm^2 resulting in individual tower acceptance of $\Delta\eta\times\Delta\phi=0.014\times0.014$ at $\eta=0$.

2.2.1. *Sampling fraction*. The present conceptual design incorporates a moderate detector average active volume density of ~5.68 g/cm^3 which results from a 1:1. 22 Pb to scintillator ratio by volume. This results in a compact detector consistent with the EMCal integration volume at the chosen detector thickness of 20.1 radiation lengths.

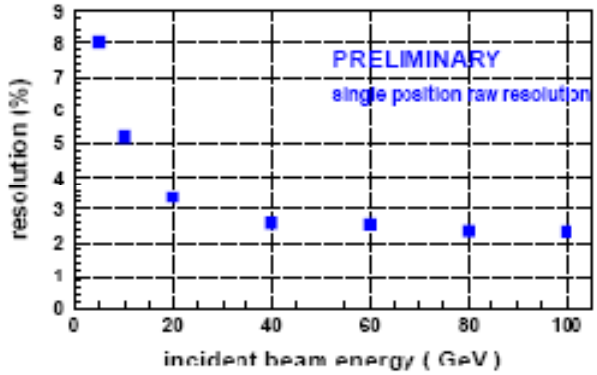

Figure 6: EMCal II generation prototype test beam results (Oct `07) for the energy resolution (no final calibration and no beam resolution subtraction).

Practical considerations, including the total assembly labor cost, suggest reducing the total number of Pb/scintillator layers thus decreasing the sampling frequency. Fig. 6 shows the measured energy resolution curve from the 16-module II generation prototype from the CERN SPS test beam (October 2007). The result was obtained using temporary calibration constants and does not include the subtraction of the beam momentum spread.

2.2.2. *Optical and Photo Sensors.* Scintillation photons produced in each tower are captured by an array of 36 Kuraray, Y-11, double clad, WLS fibers that run longitudinally through the Pb/scintillator stack (Fig. 7). Each fiber terminates in an aluminized mirror at the front face end of the module and is integrated into a polished, circular group of 36 at the photo sensor end at the back of the module. The fiber bundles are pre-fabricated and inserted into the towers after the module mechanical assembly is completed. The 36 individual fibers are packed into a circular array 6.8 mm in diameter and held in place inside a custom injection molded grommet by Bicron BC-600 optical cement. An optical quality finish is applied to the assembled bundle using a diamond polishing machine. At the other end of the bundle, individual fibers are similarly polished and mirrored with a sputtered coat of aluminum thick enough to ensure the protection of the inner mirror. The response of the Al-coated fiber is considerably flatter with an overall increase in efficiency in the range of about 25% in the vicinity of shower maximum (i.e. the location of the highest energy deposition for an electromagnetic shower). This number accounts for material immediately in front of the detector; which ranges between 0.4 and 0.8 radiation lengths, and assumes 5.5 - 6.0 radiation lengths for shower maximum for 10 GeV photons. At this depth in the detector, the mirrored fiber response is very uniform and contributes nothing significant to the non-linearity of the detector as a whole. Other factors which can significantly impact the electromagnetic performance of the calorimeter, include scintillator edge treatment and the density of the wavelength shifting fiber readout pattern and the material chosen for the interlayer diffuse reflector. For scintillator edge treatment and fiber density, advantage was taken

from the extensive studies made by the LHCb collaboration for their ECAL [12]. In particular, a diffuse reflector edge treatment was adopted, such as that obtained with Bicron Titanium Dioxide loaded white paint (BC622A) with a total fiber density of about one fiber per cm^2. In the case of the interlayer diffuse reflector, a white, acid free, bond paper was used in place of the Teflon based commercial TYVEK. While TYVEK produces slightly better surface reflectivity, its coefficient of friction is too low to permit its use in this design where the module's mechanical stability depends somewhat on the interlayer friction.

Figure 7: Fibre bundles with attached APD and preamplifier of four towers of an EMCal module.

The 6.8 mm diameter fiber bundle from a given tower connects to the APD through a short light guide/diffuser with a square cross section of 7 mm × 7 mm that tapers slowly down to 4.5 mm × 4.5 mm as it mates (glued) to the 5 mm × 5 mm active area of the photo sensor. Fig. 7 shows also 4 pre-fabricated fiber bundles inserted into the towers of a single prototype module. In this picture all of the module rear enclosing and structural elements are omitted so the convergence of the wavelength shifting fibers may be seen as they converge to the light guide (inside the black plastic tube) and finally to mate with the APD and charge sensitive preamplifier (CSP). The selected photo sensor is the Hamamatsu S8664-55 Avalanche Photo Diode. This photodiode has a peak spectral response at a wavelength of 585 nm compared to an emission peak of 476 nm for the Y-11 fibers. However, both the spectral response and the quantum efficiency of the APD are quite broad with the latter dropping from the maximum by only ~5% at the WLS fiber emission peak. At this wavelength, the manufacturer's specification gives a quantum efficiency of 80%.

3. **Module Integration to Strip Modules and Super Modules.**

As described above, the super module is the basic building block of the calorimeter. Starting with 288 individual modules which are rather compact and heavy, the main engineering task is to create a super module structure which is rigid, with small deflections in any orientation yet does not require extensive, heavy external stiffening components that would reduce the volume available for the active detector. The solution adopted for the ALICE EMCal is to develop a super module “crate” which functions not as a box for the individual modules but rather an integrated structure in which the individual elements contribute to the overall stiffness. The super module crate is effectively a large I-beam in which the flanges are the long sides of the crate and the 24 rows of strip modules together. This configuration gives to the super module good stiffness for both the 9 o'clock and 10 o'clock locations. For the 12 o'clock location, the I-beam structure of the super module is augmented by a 1

mm thick stainless steel forward sheet (traction loaded), which controls the bending moment tending to "open" the crate main sides, and helps to limit deflection of strip modules. Ridges are provided on the interior surfaces of the crate to allow precision alignment of the strip modules at the correct angle. The stiffness given by this I-beam concept allows the use of non-magnetic light alloys for main parts of the super module crate. Parts of the super module crate will be made mainly from laminated 2024 aluminum alloy plates. The two main sides (flanges of the I-beam) of the crate will be assembled from 2 plates, 25 mm and 25 mm thick, bolted together and arranged so as to approximately follow the taper of the 20 degree sector boundary. Each of the 24 rows of a super module contain 12 modules as described above. Each of the modules is attached to a transverse beam by 3.4 mm diameter stainless steel screws. The 12 modules and the transverse beam form a strip module. The strip module is 1440 mm long, 120 mm wide, 410 mm thick. The total weight of the strip module is approximately 300 kg and like module, it is a self supporting unit. The transverse beam, which is the structural part of the strip module, is made from cast aluminum alloy with individual cavities along its length where the fibers emerging from towers are allowed to converge. The casting process is well suited to forming these cavities and the overall structure, saving considerable raw material and machining time. Fig. 4 (left panel) shows the overall layout and dimensions of a strip module. In addition to functioning as a convenient structural unit which offers no interference with the active volume of the detector and forming the web of the I-beam structure of the super module, the transverse beam of the strip module provides protection for the fibers, a structural mount for the light guide, APD and charge sensitive preamplifier and a light tight enclosure for these elements.

4. Conclusions

According to the very important but not final RHIC results, jet quenching studies are the ultimate tool to probe QCD dense matter. In order to go further there is a need to measure the jet structure modification over a huge kinematic range, while having an efficient jet triggering and particle tracking and, last but not least, a detailed particle identification down to low p_T. The ALICE detector augmented with the EMCal can fully meet these demands.

References

[1] F. Carminati et al. (ALICE Collaboration), J. Phys. G30 1517 (2004).
[2] ALICE Collaboration, Physics Performace Report, Vol 2, J. Phys. G (2006).
[3] R. Baier, D. Schiff and B. Zakharov, Ann. Rev. Nucl. Part. Sci. 50, 37 (2000).
[4] M. Gyulassy, I. Vitev, X. N.Wang and B.W. Zhang, Quark Gluon Plasma 3, 123 (ed. R. Hwa and X. N. Wang, World Scientific, Singapore); nucl-th/0302077.
[5] A. Kovner and U. Wiedemann, Quark Gluon Plasma 3, 192 (ed. R. Hwa and X. N. Wang, World Scientific, Singapore); hep-ph/0304151.
[6] P. Jacobs and X. N. Wang, Prog. Part. Nucl. Phys. 54, 443 (2005).
[7] D. Buskulic et al. (ALEPH), Nucl. Instr. Meth. A360, 481 (1995).
[8] M. Miller et al. (STAR), proceedings of PANIC05, hep-ex/0604001.
[9] S. S. Adler et al. (PHENIX), Phys. Rev. C69, 034909 (2004).
[10] J. Adams et al. (STAR), nucl-ex/0601042.
[11] L. Aphecetche et. al., (PHENIX), Nucl. Instrum. Methods A499 (2003) 521.
[12] LHCB Collaboration, LHCb TDR2, CERN/LHCC 2000-36, 6 September 2000.